

## Electric dipole moment of the $\rho$ -meson

Mario Pitschmann,<sup>1,2</sup> Chien-Yeah Seng,<sup>1</sup> Michael J. Ramsey-Musolf,<sup>1,3</sup>  
 Craig D. Roberts,<sup>2,4</sup> Sebastian M. Schmidt,<sup>5</sup> and David J. Wilson<sup>2</sup>

<sup>1</sup>*University of Wisconsin-Madison, Madison, Wisconsin 53706, USA*

<sup>2</sup>*Physics Division, Argonne National Laboratory, Argonne, Illinois 60439, USA*

<sup>3</sup>*California Institute of Technology, Pasadena, California 91125, USA*

<sup>4</sup>*Department of Physics, Illinois Institute of Technology, Chicago, Illinois*

<sup>5</sup>*Institute for Advanced Simulation, Forschungszentrum Jülich and JARA, D-52425 Jülich, Germany*

(Dated: 19 September 2012)

At an hadronic scale the effect of CP-violating interactions that typically appear in extensions of the Standard Model may be described by an effective Lagrangian, in which the operators are expressed in terms of lepton and partonic gluon and quark fields, and ordered by their mass dimension,  $k \geq 4$ . Using a global-symmetry-preserving truncation of QCD's Dyson-Schwinger equations, we compute the  $\rho$ -meson's electric dipole moment (EDM),  $d_\rho$ , as generated by the leading dimension-four and -five CP-violating operators and an example of a dimension-six four-quark operator. The two dimension-five operators; viz., quark-EDM and -chromo-EDM, produce contributions to  $d_\rho$  whose coefficients are of the same sign and within a factor of two in magnitude. Moreover, should a suppression mechanism be verified for the  $\theta$ -term in any beyond-Standard-Model theory, the contribution from a four-quark operator can match the quark-EDM and -chromo-EDM in importance. This study serves as a prototype for the more challenging task of computing the neutron's EDM.

PACS numbers: 11.30.Er, 14.40.Be, 11.15.Tk, 12.60.Jv

### I. INTRODUCTION

The action for any local quantum field theory is invariant under the transformation generated by the antiunitary operator  $CPT$ , which is the product of the inversions:  $C$ , charge conjugation;  $P$ , parity transformation; and  $T$ , time reversal. The combined  $CPT$  transformation provides a rigorous correspondence between particles and antiparticles, and it relates the  $S$  matrix for any given process to its inverse, where all spins are flipped and the particles replaced by their antiparticles. Lorentz and  $CPT$  symmetry together have many consequences, amongst them, that the mass and total width of any particle are identical to those of its antiparticle.

It is within this context that the search for the intrinsic electric dipole moment (EDM) of an elementary or composite but fundamental particle has held the fascination of physicists for over sixty years [1]. Its existence indicates the simultaneous violation of parity- and time-reversal-invariance in the theory that describes the particle's structure and interactions; and the violation of  $P$ - and  $T$ -invariance entails that  $CP$  symmetry is also broken. This last is critical for our existence because we represent a macroscopic excess of matter over antimatter. As first observed by Sakharov [2], in order for a theory to explain an excess of baryon matter, it must include processes that change baryon number, and break  $C$ - and  $CP$ -symmetries; and the relevant processes must have taken place out of equilibrium, otherwise they would merely have balanced matter and antimatter. (Alternately, the presence of CPT violation can circumvent the out-of-equilibrium environment.)

The electroweak component of the Standard Model (SM) is capable of satisfying Sakharov's conditions, owing to the existence of a complex phase in the  $3 \times 3$ -CKM matrix which enables processes that mix all three quark generations. However, this high-order process is too weak to explain the observed matter-antimatter asymmetry [3–5]. Hence, it is widely expected that any description of baryogenesis will require new sources of CP violation beyond the SM. This presents little difficulty, however, because extensions of the SM typically possess  $CP$ -violating interactions, whose parameters must, in fact, be tuned to small values in order to avoid conflict with known bounds on the size of such EDMs [5–9]. (For recent analyses, see, e.g., Refs. [10–12] and references therein.)

The question here is how such bounds should be imposed. That is not a problem for elementary particles, like the electron. However, it is a challenge when the SM extension produces an operator involving current-quarks and/or gluons. In that case the  $CP$  violation is expressed as an hadronic property and one must have at hand a nonperturbative method with which to compute the impact of  $CP$ -violating features of partonic quarks and gluons on the hadronic composite.

To elucidate, extensions of the SM are typically active at some large but unspecified energy-scale,  $\Lambda$ , and their effect at an hadronic scale is expressed in a low-energy effective Lagrangian:

$$\mathcal{L}_{\text{eff}} \sim \sum_{j,k} K_j O_j^{(k)} \Lambda^{4-k}, \quad (1)$$

where  $O_j^{(k)}$  are composite  $CP$ -odd local operators of di-

mension  $k \geq 4$  and  $\{K_j\}$  are dimensionless strength parameters, which monitor the size of the model's  $CP$ -violating phases and commonly evolve logarithmically with the energy scale. The calculation of an hadronic EDM therefore proceeds in two steps. The first, easier, part requires calculation of the coefficients  $\{K_i\}$  in a given model. This involves the systematic elimination of degrees-of-freedom that are irrelevant at energy-scales less than  $\Lambda$ . The second, far more challenging exercise, is the nonperturbative problem of translating the current-quark-level interaction in Eq. (1) into observable properties of hadrons.

We illustrate the procedure in the case of the  $\rho$ -meson. Not that there is any hope of measuring a  $\rho$ -meson EDM but because the nonperturbative methods necessary can most readily be illustrated in the case of systems defined by two valence-quark degrees-of-freedom. In taking this path, we follow other authors [13–15] but will nonetheless expose novel insights, especially because we consider more operator structures than have previously been considered within a single unifying framework. It is worth remarking here that particles with spin also possess a magnetic dipole moment. That moment is aligned with the particle's spin because it is the only vector available. The same is true of the expectation value of any electric dipole moment.

Herein we shall estimate the contribution of some dimension four, five and six operators to the EDM of the  $\rho^+$ -meson; viz., the impact on the  $\rho$  of the local Lagrangian density

$$\begin{aligned} \mathcal{L}_{\text{eff}} = & -i\bar{\theta} \frac{g_s^2}{32\pi^2} G_{\mu\nu}^a \tilde{G}_{\mu\nu}^a - \frac{i}{2} \sum_{q=u,d} d_q \bar{q} \gamma_5 \sigma_{\mu\nu} q F_{\mu\nu} \\ & - \frac{i}{2} \sum_{q=u,d} \tilde{d}_q \bar{q} \frac{1}{2} \lambda^a \gamma_5 \sigma_{\mu\nu} q g_s G_{\mu\nu}^a \\ & + \frac{\mathcal{K}}{\Lambda^2} i\varepsilon_{jkl} [\bar{Q}_j d \bar{Q}_k \gamma_5 u + \text{h.c.}], \end{aligned} \quad (2)$$

where: latin superscripts represent colour;  $g_s$  is the strong coupling constant;  $F_{\mu\nu}$  and  $G_{\mu\nu}^a$  are photon and gluon field-strength tensors, respectively, and  $\tilde{G}_{\mu\nu}^a = (1/2)\epsilon_{\mu\nu\lambda\rho} G_{\lambda\rho}^a$ ;  $\{\tilde{Q}_i | i = 1, 2\} = \{\bar{u}_L, \bar{d}_L\}$ , with the subscript indicating left-handed;  $\bar{\theta}$  is QCD's effective  $\theta$ -parameter, which combines  $\theta_{\text{QCD}}$  and the unknown phase of the current-quark-mass matrix; and  $\{d_q\}$ ,  $\{\tilde{d}_q\}$  are quark EDMs and chromo-EDMs, respectively.

We note that Eq.(2) is expressed at a renormalisation scale  $\zeta \sim 2 \text{ GeV}$ , which is far below that of electroweak symmetry breaking but still within the domain upon which perturbative QCD is applicable. Moreover, we have chosen to include just one dimension-six operator in the Lagrangian; i.e., a particular type of four-fermion interaction. There is a host of dimension-six operators, Weinberg's CP-odd three-gluon vertex amongst them [16]. However, for our illustrative purpose, nothing is lost by omitting them because the potency of the one operator we do consider can serve as an indication of the

strength with which each might contribute.

One merit of our analysis of the contribution from Eq.(2) to the EDM of the  $\rho^+$ -meson is the connection of these EDM responses with values of a vast array of hadron observables that are all computed within precisely the same framework using exactly the same parameters [17–22]. We explain this framework in Sec. II. In addition to providing the first such comprehensive treatment, our study is novel in considering the impact of a dimension-six operator on the  $\rho^+$ -meson's EDM.

We introduce the  $\rho$ -meson electromagnetic form factors in Sec. III. The effects of Eq. (2) on the  $\rho$ -meson bound-state are analysed in Sec. IV. Each interaction term is considered separately, so that we present a raft of algebraic formulae that are readily combined, evaluated and interpreted. Numerical results are provided in Sec. V and placed in context with previous studies. Section VI is an epilogue.

## II. $\rho$ -MESON AS A BOUND STATE

### A. $\rho$ - $\gamma$ Vertex

The  $\rho^+$ -meson is a composite particle and thus its EDM appears in the dressed vertex that describes its coupling with the photon; viz.,

$$\begin{aligned} & \mathcal{P}_{\alpha\alpha'}^T(p) \Gamma_{\alpha'\mu\beta'}(p, p') \mathcal{P}_{\beta'\beta}^T(p') \\ & = \mathcal{P}_{\alpha\alpha'}^T(p) \left\{ (p + p')_\mu [-\delta_{\alpha'\beta'} \mathcal{E}(q^2) + q_{\alpha'} q_{\beta'} \mathcal{Q}(q^2)] \right. \\ & \quad - (\delta_{\mu\alpha'} q_{\beta'} - \delta_{\mu\beta'} q_{\alpha'}) \mathcal{M}(q^2) \\ & \quad \left. - i\varepsilon_{\alpha'\beta'\mu\sigma} q_\sigma \mathcal{D}(q^2) \right\} \mathcal{P}_{\beta'\beta}^T(p'), \end{aligned} \quad (3)$$

where:  $p_\alpha$  is the momentum of the incoming  $\rho$ -meson;  $p'_{\beta'}$ , that of the outgoing  $\rho$ ;  $q_\mu = p'_\mu - p_\mu$ ; and

$$\mathcal{P}_{\alpha\beta}^T(p) = \delta_{\alpha\beta} - \frac{p_\alpha p_\beta}{p^2}. \quad (4)$$

The vertex involves four scalar form factors whose  $q^2 = 0$  values are understood as follows:  $\mathcal{E}(0)$ , electric charge, which is “1” in this case;  $\mathcal{M}(0)$ , magnetic moment,  $\mu_\rho$ , in units of  $e/[2m_\rho]$ , where  $e$  is the magnitude of the electron charge;  $\mathcal{Q}(0) = (2/m_\rho^2)(Q_\rho + \mu_\rho - 1)$ , with  $Q_\rho$  the meson's electric quadrupole moment; and  $\mathcal{D}(0)$  is the meson's electric dipole moment, in units of  $e/[2m_\rho]$ .

### B. Contact Interaction

Our goal is calculation of the last of these,  $\mathcal{D}(0)$ , and for this we choose to work within the continuum framework provided by QCD's Dyson-Schwinger equations (DSEs) [23–25]. To be specific, we perform the computation using a global-symmetry-preserving treatment of a vector  $\times$  vector contact-interaction because that has proven to be a reliable explanatory and predictive

tool for hadron properties measured with probe momenta less-than the dressed-quark mass,  $M \sim 0.4 \text{ GeV}$  [17–22].

To expand upon the reasons for this choice of interaction we note that DSE kernels with a closer connection to perturbative QCD; namely, which preserve QCD’s one-loop renormalisation group behaviour, have long been employed in studies of the spectrum and interactions of mesons [26–28]. Such kernels are developed in the rainbow-ladder approximation, which is the leading-order in a systematic and global-symmetry-preserving truncation scheme [29, 30]; and their model input is expressed via a statement about the nature of the gap equation’s kernel at infrared momenta. With a single parameter that expresses a confinement length-scale or strength [31, 32], they have successfully described and predicted numerous properties of vector [32–36] and pseudoscalar mesons [32, 35–40] with masses less than 1 GeV, and ground-state baryons [41–44]. Such kernels are also reliable for ground-state heavy-heavy mesons [45]. Given that contact-interaction results for low-energy observables are indistinguishable from those produced by the most sophisticated interactions, it is sensible to capitalise on the simplicity of the contact-interaction herein.

The starting point for our study is the dressed-quark propagator, which is obtained from the gap equation:

$$S(p)^{-1} = i\gamma \cdot p + m + \int \frac{d^4q}{(2\pi)^4} g^2 D_{\mu\nu}(p-q) \frac{\lambda^a}{2} \gamma_\mu S(q) \frac{\lambda^a}{2} \Gamma_\nu(q, p), \quad (5)$$

wherein  $m$  is the Lagrangian current-quark mass,  $D_{\mu\nu}$  is the vector-boson propagator and  $\Gamma_\nu$  is the quark–vector-boson vertex. We use

$$g^2 D_{\mu\nu}(p-q) = \delta_{\mu\nu} \frac{4\pi\alpha_{\text{IR}}}{m_G^2}, \quad (6)$$

where  $m_G = 0.8 \text{ GeV}$  is a gluon mass-scale typical of the one-loop renormalisation-group-improved interaction introduced in Ref. [35], and the fitted parameter  $\alpha_{\text{IR}}/\pi = 0.93$  is commensurate with contemporary estimates of the zero-momentum value of a running-coupling in QCD [46, 47]. Equation (6) is embedded in a rainbow-ladder truncation of the DSEs, which is the leading-order in the most widely used, symmetry-preserving truncation scheme [30]. This means

$$\Gamma_\nu(p, q) = \gamma_\nu \quad (7)$$

in Eq.(5) and in the subsequent construction of the Bethe-Salpeter kernels. One may view the interaction in Eq. (6) as being inspired by models of the Nambu–Jona-Lasinio (NJL) type [48]. However, in implementing the interaction as an element in a rainbow-ladder truncation of the DSEs, our treatment is atypical; e.g., we have a single, unique coupling parameter, whereas common applications of the NJL model have different, tunable strength parameters for each collection of operators that mix under symmetry transformations.

Using Eqs. (6), (7), the gap equation becomes

$$S^{-1}(p) = i\gamma \cdot p + m + \frac{16\pi}{3} \frac{\alpha_{\text{IR}}}{m_G^2} \int \frac{d^4q}{(2\pi)^4} \gamma_\mu S(q) \gamma_\mu, \quad (8)$$

an equation in which the integral possesses a quadratic divergence, even in the chiral limit. When the divergence is regularised in a Poincaré covariant manner, the solution is

$$S(p)^{-1} = i\gamma \cdot p + M, \quad (9)$$

where  $M$  is momentum-independent and determined by

$$M = m + M \frac{4\alpha_{\text{IR}}}{3\pi m_G^2} \int_0^\infty ds s \frac{1}{s + M^2}. \quad (10)$$

Our regularisation procedure follows Ref. [49]; i.e., we write

$$\begin{aligned} \frac{1}{s + M^2} &= \int_0^\infty d\tau e^{-\tau(s+M^2)} \\ &\rightarrow \int_{\tau_{\text{uv}}^2}^{\tau_{\text{ir}}^2} d\tau e^{-\tau(s+M^2)} \end{aligned} \quad (11)$$

$$= \frac{e^{-(s+M^2)\tau_{\text{uv}}^2} - e^{-(s+M^2)\tau_{\text{ir}}^2}}{s + M^2}, \quad (12)$$

where  $\tau_{\text{ir}, \text{uv}}$  are, respectively, infrared and ultraviolet regulators. It is apparent from Eq. (12) that  $\tau_{\text{ir}} =: 1/\Lambda_{\text{ir}}$  finite implements confinement by ensuring the absence of quark production thresholds [23, 50]. Since Eq. (6) does not define a renormalisable theory, then  $\Lambda_{\text{uv}} := 1/\tau_{\text{uv}}$  cannot be removed but instead plays a dynamical role, setting the scale of all dimensioned quantities.

Using Eq. (11), the gap equation becomes

$$M = m + M \frac{4\alpha_{\text{IR}}}{3\pi m_G^2} \mathcal{C}^{\text{iu}}(M^2), \quad (13)$$

where

$$\mathcal{C}^{\text{iu}}(M^2) = M^2 \bar{\mathcal{C}}^{\text{iu}}(M^2) \quad (14)$$

$$= M^2 [\Gamma(-1, M^2 \tau_{\text{uv}}^2) - \Gamma(-1, M^2 \tau_{\text{ir}}^2)], \quad (15)$$

with  $\Gamma(\alpha, y)$  the incomplete gamma-function, and, for later use,  $\mathcal{C}_1^{\text{iu}}(z) = -z(d/dz)\mathcal{C}^{\text{iu}}(z)$ .

In rainbow-ladder truncation, with the interaction in Eq. (6), the homogeneous Bethe-Salpeter equation for the colour-singlet  $\rho$ -meson is

$$\Gamma_\mu^\rho(k; P) = -\frac{16\pi}{3} \frac{\alpha_{\text{IR}}}{m_G^2} \int \frac{d^4q}{(2\pi)^4} \gamma_\sigma \chi_\mu^\rho(q; P) \gamma_\sigma, \quad (16)$$

where  $\chi_\mu^\rho(q; P) = S(q+P)\Gamma_\mu^\rho(q; P)S(q)$  and  $\Gamma_\mu(q; P)$  is the meson’s Bethe-Salpeter amplitude. Since the integrand does not depend on the external relative-momentum,  $k$ , then a global-symmetry-preserving regularisation of Eq. (16) yields solutions that are independent of  $k$ . With a dependence on the relative momentum

TABLE I. Results obtained with  $\alpha_{\text{IR}}/\pi = 0.93$  and (in GeV):  $m = 0.007$ ,  $\Lambda_{\text{ir}} = 0.24$ ,  $\Lambda_{\text{uv}} = 0.905$  [20]. The Bethe-Salpeter amplitudes are canonically normalised;  $\kappa_\pi$  is the pion condensate [51–53]; and  $f_{\pi,\rho}$  are the mesons’ leptonic decay constants. Empirical values are  $\kappa_\pi \approx (0.22 \text{ GeV})^3$  and [54]  $f_\pi = 0.092 \text{ GeV}$ ,  $f_\rho = 0.153 \text{ GeV}$ . All dimensioned quantities are listed in GeV.

$E_\pi$	$F_\pi$	$E_\rho$	$M$	$\kappa_\pi^{1/3}$	$m_\pi$	$m_\rho$	$f_\pi$	$f_\rho$
3.639	0.481	1.531	0.368	0.243	0.140	0.929	0.101	0.129

forbidden by the interaction, then the rainbow-ladder vector-meson Bethe-Salpeter amplitude takes the form

$$\Gamma_\mu^\rho(P) = \gamma_\mu^T E_\rho(P), \quad (17)$$

where  $P_\mu \gamma_\mu^T = 0$ ,  $\gamma_\mu^T + \gamma_\mu^L = \gamma_\mu$ . We assume isospin symmetry throughout and hence do not explicitly include the Pauli isospin matrices.<sup>1</sup>

Values of some meson-related quantities, of relevance herein and computed using the contact-interaction, are reported in Table I. We quote pion properties in order to provide a broader picture: the pion’s Bethe-Salpeter amplitude is

$$\Gamma^\pi(P) = \gamma_5 \left[ iE_\pi(P) + \frac{1}{M} \gamma \cdot P F_\pi(P) \right]. \quad (18)$$

### III. $\rho$ -MESON FORM FACTORS

At this point we can proceed to computation of the form factors. In order to ensure a symmetry-preserving treatment, one must calculate the vertex in Eq. (3) at the same level of approximation as used for the dressed-quark propagator and meson Bethe-Salpeter amplitude; i.e., the generalised impulse approximation:

$$\Gamma_{\alpha\mu\beta}(p, p') = \Gamma_{\alpha\mu\beta}^u(p, p') + \Gamma_{\alpha\mu\beta}^d(p, p'), \quad (19)$$

$$\Gamma_{\alpha\mu\beta}^f(p, p') = 2 \int \frac{d^4 k}{(2\pi)^4} \text{Tr}_{CD} \left\{ i\Gamma_\beta^{\rho j}(k; -p') S(k_{++}) \right. \\ \left. \times i\Gamma_\mu^f(k_{-+}, k_{++}) S(k_{-+}) i\Gamma_\alpha^{\rho j}(k - q/2; p) S(k_{--}) \right\}, \quad (20)$$

wherein the trace is over colour and spinor indices and  $k_{\alpha\beta} = k + \alpha q/2 + \beta p/2$ . We illustrate Eq. (20) in Fig. 1.

In evaluating Eq. (19) we write:

$$S_f = S + \delta_{\text{CP}} S_f, \quad f = u, d, \quad (21)$$

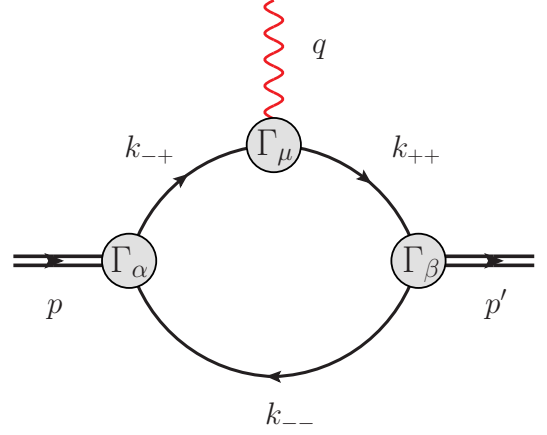


FIG. 1. Impulse approximation to the  $\rho$ - $\gamma$  vertex, Eq. (20): solid lines – dressed-quark propagators; and shaded circles, clockwise from top – Bethe-Salpeter vertex for quark-photon coupling, and Bethe-Salpeter amplitudes for the  $\rho^+$ -meson.

where  $S$  is given in Eq. (9), with the dressed-mass obtained from Eq. (10), and the broken- $CP$  corrections  $\delta_{\text{CP}} S_f$  are detailed below; and the  $\rho$ -amplitude

$$\Gamma_\alpha^{\rho j} = \gamma_\alpha^T E_\rho(P) + \Gamma_\alpha^{\rho j \text{CP}}, \quad (22)$$

with  $E_\rho(P)$  explained in connection with Eq. (17) and the broken- $CP$  corrections  $\Gamma_\alpha^{\rho j \text{CP}}$  explained below. Our computed values for the dressed-quark mass,  $M$ , and  $E_\rho$  are listed in Table I.

The remaining element in Eq. (19) is the dressed-quark–photon vertex. We are only interested in the  $q^2 = 0$  values of the form factors and hence may use

$$e\Gamma_\mu(p_1, p_2) = e\tilde{Q}\gamma_\mu + i\tilde{\mathcal{D}}\gamma_5\sigma_{\mu\nu}(p_2 - p_1)_\nu \quad (23)$$

$$=: e \text{diag}[e_u \Gamma_\mu^u(p_1, p_2), -e_d \Gamma_\mu^d(p_1, p_2)], \quad (24)$$

where  $e$  is the positron charge,  $\tilde{Q} = \text{diag}[e_u = 2/3, -e_d = 1/3]$  and  $\tilde{\mathcal{D}} = \text{diag}[d_u, -d_d]$ , with  $d_f$  the EDM of a current quark with flavour  $f$ . N.B. The second term in Eq. (23) describes the explicit current-quark EDM interaction in Eq. (2). In Sec. IV we show that the other terms in Eq. (2) generate additional contributions that interfere with this explicit term.

Note that both structures in the vertex, Eq. (23), are in general multiplied by momentum-dependent scalar functions. Naturally, the vector Ward-Takahashi identity ensures that the coefficient of the  $\tilde{Q}\gamma_\mu$  term is “1” at  $q^2 = 0$ . In connection with the tensor term, one knows from Ref. [20] that a tensor vertex is not dressed in the rainbow-ladder treatment of the contact interaction. However, with a more sophisticated interaction, strong interaction dressing of the  $\gamma_5\sigma_{\mu\nu}$  part of the quark-photon vertex might be significant, given that the dressed-quark-photon vertex certainly possesses a large dressed-quark anomalous magnetic moment term owing to dynamical chiral symmetry breaking [55]. At  $q^2 = 0$ , this could enhance the strength of the  $\tilde{\mathcal{D}}$  term by as much

<sup>1</sup> Note, too, that we use a Euclidean metric:  $\{\gamma_\mu, \gamma_\nu\} = 2\delta_{\mu\nu}$ ;  $\gamma_\mu^\dagger = \gamma_\mu$ ;  $\gamma_5 = \gamma_4\gamma_1\gamma_2\gamma_3$ ,  $\text{tr}[\gamma_5\gamma_\mu\gamma_\nu\gamma_\rho\gamma_\sigma] = -4\epsilon_{\mu\nu\rho\sigma}$ ;  $\sigma_{\mu\nu} = (i/2)[\gamma_\mu, \gamma_\nu]$ ;  $a \cdot b = \sum_{i=1}^4 a_i b_i$ ; and  $P_\mu$  timelike  $\Rightarrow P^2 < 0$ .

as a factor of ten. If so, then sensitivity to current-quark EDMs is greatly magnified. It is worth bearing this in mind.

Working with Eq. (3), it is sufficient herein to employ three projection operators:

$$P_{\alpha\mu\beta}^1 = \mathcal{P}_{\alpha\sigma}^T(p) P_{\mu} P_{\sigma\beta}^T(p'), \quad (25a)$$

$$P_{\alpha\mu\beta}^2 = \mathcal{P}_{\alpha\alpha'}^T(p) \mathcal{P}_{\beta'\beta}^T(p') \left( \frac{\delta_{\mu\beta'} q_{\alpha'} - \delta_{\mu\alpha'} q_{\beta'}}{q^2} + \frac{P_{\mu} \delta_{\alpha'\beta'}}{6p^2} \right), \quad (25b)$$

$$P_{\alpha\mu\beta}^3 = \frac{1}{2iq^2} \mathcal{P}_{\alpha\alpha'}^T(p) \varepsilon_{\alpha'\beta'\mu\sigma} q_{\sigma} \mathcal{P}_{\beta'\beta}^T(p'), \quad (25c)$$

with  $p' = p + q$ ,  $P = p + p'$ , for then

$$\mathcal{E}(0) = \lim_{q^2 \rightarrow 0} \frac{1}{12m_{\rho}^2} P_{\alpha\mu\beta}^1 \Gamma_{\alpha\mu\beta}, \quad (26a)$$

$$\mathcal{M}(0) = \lim_{q^2 \rightarrow 0} \frac{1}{4} P_{\alpha\mu\beta}^2 \Gamma_{\alpha\mu\beta}, \quad (26b)$$

$$\mathcal{D}(0) = \lim_{q^2 \rightarrow 0} P_{\alpha\mu\beta}^3 \Gamma_{\alpha\mu\beta}, \quad (26c)$$

and  $\mu_{\rho} = \mathcal{M}(0) e/[2m_{\rho}]$ ,  $d_{\rho} = \mathcal{D}(0) e/[2m_{\rho}]$ . So long as a global-symmetry-preserving regularisation scheme is implemented,  $\mathcal{E}(0) = 1$ ; the value of  $\mathcal{M}(0)$  is then a prediction, which can both be compared with that produced by other authors and serve as a benchmark for our prediction of  $\mathcal{D}(0)$ .

At this point one has sufficient information to calculate the  $\rho$ -meson's magnetic moment. We simplify the denominator in Eq. (19) via a Feynman parametrisation:

$$\begin{aligned} & (k_{++}^2 + M^2)^{-1} (k_{-+}^2 + M^2)^{-1} (k_{--}^2 + M^2)^{-1} \\ &= 2 \int_0^1 \int_0^{1-x} dx dy \left[ k^2 + M^2 \right. \\ & \quad \left. + \frac{1}{4} [p^2 - 2(1-2x-2y)p \cdot q + q^2] \right. \\ & \quad \left. - (1-2y)q \cdot k + (1-2x)p \cdot k \right]^{-3}. \end{aligned} \quad (27)$$

This appears as part of an expression that is integrated over four-dimensional  $k$ -space. The expression is simplified by a shift in integration variables, which exposes a denominator of the form  $1/[k^2 + \tilde{M}^2]^3$ , with

$$\tilde{M}^2 = M^2 + x(x-1)m_{\rho}^2 + y(1-x-y)Q^2. \quad (28)$$

One thereby arrives at a compound expression that involves one-dimensional integrals of the form in Eq. (10), which we regularise via Eq. (11) and generalisations thereof; viz.,

$$\int ds \frac{s}{[s+\omega]^2} = -\frac{d}{d\omega} C^{\text{iu}}(\omega) =: \bar{C}_1^{\text{iu}}(\omega), \quad (29a)$$

$$\int ds \frac{s}{[s+\omega]^3} = \frac{1}{2} \frac{d^2}{d\omega^2} C^{\text{iu}}(\omega) =: \bar{C}_2^{\text{iu}}(\omega), \quad (29b)$$

$$\int ds \frac{s^2}{[s+\omega]^3} = \bar{C}_1^{\text{iu}}(\omega) - \omega \bar{C}_2^{\text{iu}}(\omega), \quad (29c)$$

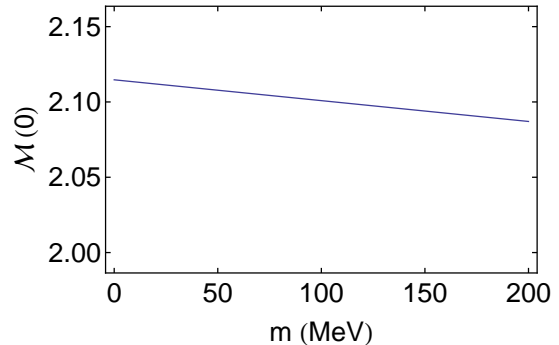


FIG. 2. Evolution of  $\rho$ -meson magnetic moment with current-quark mass.  $m = 170$  MeV corresponds to the mass of the  $s$ -quark in our treatment of the contact interaction [22], so the difference between  $\mathcal{M}_{\rho}(0)$  and  $\mathcal{M}_{\phi}(0)$  is just 1%.

etc. Details for this component of our computation may be found in Ref. [20] and pursuing it to completion one obtains the magnetic moment listed in Table II.

We depict the evolution of  $\mathcal{M}(0)$  with current-quark mass in Fig. 2:  $\mathcal{M}(0)$  is almost independent of  $m$ . This outcome matches that obtained in Ref. [34] using a renormalisation-group-improved one-gluon exchange kernel and hence a momentum-dependent dressed-quark mass-function of the type possessed by QCD [60–63]. The behaviour in Fig. 2 will serve to benchmark that of the  $\rho$ -meson's EDM.

#### IV. $\rho$ -MESON EDM: FORMULAE

We now turn to computation of the effect of the interaction terms in Eq. (2) on the  $\rho$ -meson. There are three types of contribution, which arise separately through modification of: (1) the quark-photon vertex, Eq. (23);

TABLE II. Magnetic moment of the  $\rho$ -meson calculated using our framework; and a comparison with other computations. Legend: *RL RGI-improved*, treatment of a renormalisation-group-improved one-gluon exchange kernel in rainbow-ladder truncation; *EF parametrisation*, entire function parametrisation of solutions to the gap and Bethe-Salpeter equations; and *LF CQM*, light-front constituent-quark model. The results are listed in units of  $e/[2m_{\rho}]$ .

This work and Ref. [20]	2.11
DSE: RL RGI-improved [34]	2.01
DSE: EF parametrisation [56]	2.69
LF CQM [57]	2.14
LF CQM [58]	1.92
Sum Rules [59]	$1.8 \pm 0.3$
point particle	2



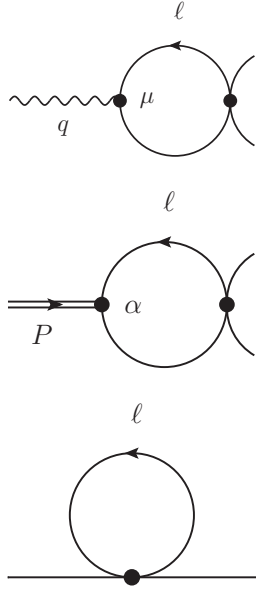


FIG. 3. *Top* – Correction to the quark-photon vertex generated by the four-fermion operator in Eq. (30). The unmodified quark-photon vertex is the left dot, whereas the right dot locates insertion of  $\mathcal{L}_6$ . If the internal line represents a circulating  $d$ -quark then, owing to the  $\mathcal{L}_6$  insertion, the external lines are  $u$ -quarks, and vice versa. *Middle* – Analogous correction to the  $\rho$ -meson Bethe-Salpeter amplitude. The unmodified amplitude is the left dot, whereas the right dot locates insertion of  $\mathcal{L}_6$ . The lower internal line is an incoming  $d$ -quark and the upper external line is an outgoing  $u$ -quark. *Bottom* –  $\mathcal{L}_6$ -correction to the dressed-quark propagator, with the dot locating the operator insertion. If the outer line is a  $u$ -quark, then the internal line is a  $d$ -quark; and vice versa.

(2) the  $\rho$ -meson Bethe-Salpeter amplitude, Eq. (22); and  
(3) the dressed-quark propagator, Eq. (21).

### A. Four-fermion interaction

We begin with the dimension-six operator, which can be written explicitly as

$$\mathcal{L}_6 = i \frac{\mathcal{K}}{2\Lambda^2} [\bar{u}^a d^a \bar{d}^b \gamma_5 u^b + \bar{u}^a \gamma_5 d^a \bar{d}^b u^b - \bar{d}^a d^a \bar{u}^b \gamma_5 u^b - \bar{d}^a \gamma_5 d^a \bar{u}^b u^b], \quad (30)$$

with summation over the repeated colour indices. This operator generates all three types of modification.

#### 1. $\mathcal{L}_6$ – quark-photon vertex

This contribution is depicted in the top panel of Fig. 3. Consider first the case of  $d$ -quarks circulating in the loop, then straightforward but careful analysis of the induced

Wick contractions produces the following result:

$$\Gamma_\mu^{\gamma_\mu d} = -i \frac{\mathcal{K}}{\Lambda^2} \frac{e_d}{e_u} \int \frac{d^4 \ell}{(2\pi)^4} [I_\mu^{12} + N_c I_\mu^3], \quad (31a)$$

$$I_\mu^{12} = -P_R S(\ell + q) \gamma_\mu S(\ell) P_R + P_L S(\ell + q) \gamma_\mu S(\ell) P_L, \quad (31b)$$

$$I_\mu^3 = P_L \text{tr}\{S(\ell + q) \gamma_\mu S(\ell) P_L\} - P_R \text{tr}\{S(\ell + q) \gamma_\mu S(\ell) P_R\}, \quad (31c)$$

where  $P_{R,L} = (1/2)(1 \pm \gamma_5)$ . These right- and left-handed projection operators satisfy  $P_R + P_L = I_D$ .

Further simplification of the integrand reveals

$$I_\mu^{12} = I_\mu^1 + I_\mu^2 = \frac{i\gamma \cdot q}{(\ell + q)^2 + M^2} \gamma_\mu \frac{M}{\ell^2 + M^2} \gamma_5 \quad (32a)$$

$$+ 2i \frac{\ell_\mu}{(\ell + q)^2 + M^2} \frac{M}{\ell^2 + M^2} \gamma_5, \quad (32b)$$

$$I_\mu^3 = \frac{2i(2\ell_\mu + q_\mu)}{(\ell + q)^2 + M^2} \frac{M}{\ell^2 + M^2} \gamma_5, \quad (32c)$$

so that one may subsequently obtain

$$\int \frac{d^4 \ell}{(2\pi)^4} I_\mu^1 = (q_\mu + i\sigma_{\mu\nu} q_\nu) \gamma_5 \times \frac{iM}{16\pi^2} \int_0^1 dx \bar{C}_1^{\text{iu}}(\omega_q), \quad (33a)$$

$$\int \frac{d^4 \ell}{(2\pi)^4} I_\mu^2 = -q_\mu \gamma_5 \frac{iM}{8\pi^2} \int_0^1 dx x \bar{C}_1^{\text{iu}}(\omega_q), \quad (33b)$$

$$\int \frac{d^4 \ell}{(2\pi)^4} I_\mu^3 = q_\mu \gamma_5 \frac{iM}{8\pi^2} \int_0^1 dx (1 - 2x) \bar{C}_1^{\text{iu}}(\omega_q), \quad (33c)$$

where  $\omega_q = x(1-x)q^2 + M^2$ . Combining the terms, Eq. (31a) becomes

$$\Gamma_\mu^{\gamma_\mu d} = \frac{\mathcal{K}}{\Lambda^2} \frac{e_d}{e_u} \frac{M}{16\pi^2} \int_0^1 dx \bar{C}_1^{\text{iu}}(\omega_q) \times [(1 + 2N_c)(1 - 2x)q_\mu + i\sigma_{\mu\nu} q_\nu] \gamma_5 \quad (34)$$

$$q^2=0 \frac{\mathcal{K}}{\Lambda^2} \frac{e_d}{e_u} \frac{M}{16\pi^2} \bar{C}_1^{\text{iu}}(M^2) i\sigma_{\mu\nu} q_\nu \gamma_5. \quad (35)$$

In the other case, with a  $u$ -quark circulating in the loop, one obtains

$$\Gamma_\mu^{\gamma_\mu u} \stackrel{q^2=0}{=} \frac{\mathcal{K}}{\Lambda^2} \frac{e_u}{e_d} \frac{M}{16\pi^2} \bar{C}_1^{\text{iu}}(M^2) i\sigma_{\mu\nu} q_\nu \gamma_5. \quad (36)$$

Plainly, the net correction to the quark-photon vertex can now be cast in the form of the second term in Eq. (23) and hence is readily expressed in  $\mathcal{D}(0)$ .

#### 2. $\mathcal{L}_6$ – Bethe-Salpeter amplitude

This correction is depicted in the middle panel of Fig. 3. Each of the four terms in Eq. (30) generates a distinct

contribution. That from the first and second are:

$$\Gamma_{\alpha}^{\rho L_6^1} = -i \frac{\mathcal{K}}{\Lambda^2} N_c E_{\rho} P_R \times \text{tr} \int \frac{d^4 \ell}{(2\pi)^4} S(\ell) P_R S(\ell + P) \gamma_{\alpha}^T, \quad (37a)$$

$$\Gamma_{\alpha}^{\rho L_6^2} = -i \frac{\mathcal{K}}{\Lambda^2} E_{\rho} P_R \times \int \frac{d^4 \ell}{(2\pi)^4} S(\ell + P) \gamma_{\alpha}^T S(\ell) P_R. \quad (37b)$$

The third and fourth terms are identical, up to sign-change and the replacement  $P_R \rightarrow P_L$ ; and hence

$$\Gamma_{\alpha}^{\rho L_6} = i \frac{\mathcal{K}}{\Lambda^2} E_{\rho} \int \frac{d^4 \ell}{(2\pi)^4} [I_{\alpha}^{12T} + N_c I_{\alpha}^{3T}], \quad (38)$$

where the superscript ‘‘T’’ indicates that  $\gamma_{\alpha}^T$  is here used in the expressions for  $I^{12}$ ,  $I^3$ .

Now, using the formulae of Sec. IV A 1, one arrives at

$$\Gamma_{\alpha}^{\rho L_6} = -i \frac{\mathcal{K}}{\Lambda^2} \frac{M E_{\rho}}{16\pi^2} \gamma_5 \sigma_{\alpha\nu} P_{\nu} \int_0^1 dx \bar{C}_1^{\text{iu}}(\omega_P), \quad (39)$$

where  $\omega_P = x(1-x)P^2 + M^2$ ,  $P^2 = -m_{\rho}^2$ . This is one of the additive corrections to the Bethe-Salpeter amplitude anticipated in Eq. (22).

### 3. $L_6$ - quark propagator

The final modification arising from the dimension-six operator is that depicted in the bottom panel of Fig. 3. So long as the correction is small, it modifies the dressed-quark propagator as follows:

$$S(k) \rightarrow S(k) + \delta_{L_6} S(k) = S(k) + S(k) i \Gamma^{S L_6} S(k), \quad (40)$$

where, once again, each of the four terms in Eq. (30) contributes. Their sum is

$$\Gamma^{S L_6} = \frac{\mathcal{K}}{\Lambda^2} \int \frac{d^4 \ell}{(2\pi)^4} [P_R S(\ell) P_R - P_L S(\ell) P_L + N_c P_R \text{tr}\{S(\ell) P_R\} - N_c P_L \text{tr}\{S(\ell) P_L\}]. \quad (41)$$

Now

$$\begin{aligned} P_R S(\ell) P_R - P_L S(\ell) P_L &= \frac{M}{\ell^2 + M^2} \gamma_5 \\ &= \frac{1}{2} [P_R \text{tr}\{S(\ell) P_R\} - P_L \text{tr}\{S(\ell) P_L\}], \end{aligned} \quad (42)$$

so that with little additional algebra one arrives at

$$\delta_{L_6} S(k) = \frac{i}{k^2 + M^2} (1 + 2N_c) \frac{\mathcal{K}}{\Lambda^2} \frac{M}{16\pi^2} C^{\text{iu}}(M^2) \gamma_5. \quad (43)$$

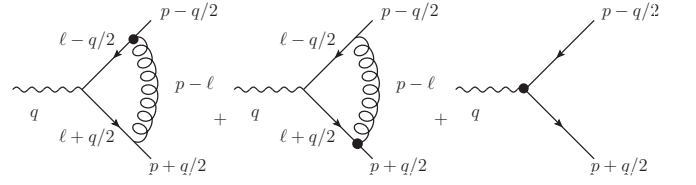


FIG. 4. Correction to the quark-photon vertex generated by the quark chromo-EDM operator in Eq. (2): the incoming and outgoing quark lines have the same flavour,  $f$ . The dot in the left two diagrams locates insertion of  $\mathcal{L}_{CEDM}$ , whilst that in the rightmost diagram indicates the second term in Eq. (23); i.e., the explicit quark EDM.

## B. Quark chromo-EDM

The term in the middle line of Eq. (2) also generates all three types of modification described in the opening lines of this Section. Notably, owing to dynamical chiral symmetry breaking, the dressed-quark-gluon coupling possesses a chromomagnetic moment term that, at infrared momenta, is two orders-of-magnitude larger than the perturbative estimate [55]. One may reasonably expect similar strong-interaction dressing of a light-quark’s chromo-EDM interaction with a gluon, in which case sensitivity to the current-quark’s chromo-EDM is very much enhanced.

### 1. $\mathcal{L}_{CEDM}$ - quark-photon vertex

This contribution is depicted in Fig. 4. After a lengthy analysis, in which we represent the exchanged gluon via Eq. (6), the sum of the two leftmost diagrams produces

$$\begin{aligned} \Gamma_{\mu}^{\gamma(g)} &= \frac{1}{6i\pi} \frac{\tilde{d}_f \alpha_{\text{IR}}}{m_G^2} \int_0^1 dx [C^{\text{iu}}(\omega_q) - C_1^{\text{iu}}(\omega_q)] \\ &\quad \times \left\{ 2q_{\alpha} \sigma_{\mu\alpha} \gamma_5 - 6i [3(x-1/2)q_{\mu} - p_{\mu}] \gamma_5 \right\} \\ &\quad - \frac{1}{3\pi} \frac{\tilde{d}_f \alpha_{\text{IR}}}{m_G^2} \int_0^1 dx \bar{C}_1^{\text{iu}}(\omega_q) \left\{ 6[\omega_q - 2M^2] p_{\mu} \gamma_5 \right. \\ &\quad - 6[(x-1/2)\omega_q + 2x(1-x)q \cdot p] q_{\mu} \gamma_5 \\ &\quad + M [((x-1/2)q + p) \cdot \gamma] q_{\alpha} \sigma_{\alpha\mu} \gamma_5 \\ &\quad \left. + M q_{\alpha} \sigma_{\alpha\mu} \gamma_5 [((x-1/2)q + p) \cdot \gamma] \right\}, \end{aligned} \quad (44)$$

where, again,  $\tilde{d}_f$  is the chromo-EDM of a quark with flavour  $f$ .

As we are interested solely in the EDM, we may con-

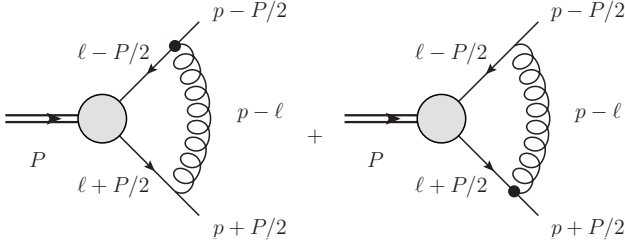


FIG. 5. Correction to the  $\rho$ -meson Bethe-Salpeter amplitude generated by the quark chromo-EDM operator in Eq. (2): the incoming line is a  $d$ -quark and the outgoing line is a  $u$ -quark. In each case the dot locates insertion of  $\mathcal{L}_{CEDM}$ .

sider  $q^2 = 0$ , at which value the result simplifies greatly:

$$\begin{aligned} \Gamma_\mu^{\gamma(g)} &= \frac{1}{3i\pi} \frac{\tilde{d}_f \alpha_{\text{IR}}}{m_G^2} [\mathcal{C}^{\text{iu}}(M^2) - \mathcal{C}_1^{\text{iu}}(M^2)] \\ &\quad \times [\gamma_5 \sigma_{\mu\alpha} q_\alpha + 3ip_\mu \gamma_5] \\ &+ \frac{1}{3\pi} \frac{\tilde{d}_f \alpha_{\text{IR}}}{m_G^2} \bar{\mathcal{C}}_1^{\text{iu}}(M^2) \left[ M \{ \gamma \cdot p, \gamma_5 \sigma_{\mu\alpha} \} q_\alpha \right. \\ &\quad \left. + 2p \cdot qq_\mu \gamma_5 + 6M^2 p_\mu \gamma_5 \right]. \end{aligned} \quad (45)$$

Plainly, the net correction to the quark-photon vertex from these two diagrams can now be cast in the form of the second term in Eq. (23), which, in fact, is precisely the rightmost diagram in Fig. 4 because  $q = p_2 - p_1$ .

## 2. $\mathcal{L}_{CEDM}$ - Bethe-Salpeter amplitude

This correction is expressed in Fig. 5. Owing to similarity between the  $\mathcal{L}_{\text{eff}}$ -uncorrected  $\rho$ -meson amplitude and quark-photon vertex, the results can be read from those in Sec. IV B 1; viz., with  $\tilde{d}_\pm = \tilde{d}_u \pm \tilde{d}_d$ ,

$$\begin{aligned} \Gamma_\alpha^{\rho(g)} &= \frac{1}{6i\pi} \frac{\alpha_{\text{IR}}}{m_G^2} E_\rho \int_0^1 dx [\mathcal{C}^{\text{iu}}(\omega_P) - \mathcal{C}_1^{\text{iu}}(\omega_P)] \\ &\quad \times \left\{ [(\tilde{d}_+ - 3(x-1/2)\tilde{d}_-)P_\beta - \tilde{d}_- p_\beta] \sigma_{\mu\beta} \gamma_5 \mathcal{P}_{\mu\alpha}^T \right. \\ &\quad \left. + 3i\tilde{d}_+ p_\mu \gamma_5 \mathcal{P}_{\mu\alpha}^T - 3\tilde{d}_- M \gamma_\mu \gamma_5 \mathcal{P}_{\mu\alpha}^T \right\} \\ &- \frac{1}{3\pi} \frac{\alpha_{\text{IR}}}{m_G^2} E_\rho \int_0^1 dx \bar{\mathcal{C}}_1^{\text{iu}}(\omega_P) \\ &\quad \times \left\{ 3\tilde{d}_+ [\omega_P - 2M^2] p_\mu \gamma_5 \mathcal{P}_{\mu\alpha}^T \right. \\ &\quad - \tilde{d}_- [(\omega_P - 2M^2)[(x-1/2)P_\beta + p_\beta]] i\gamma_5 \sigma_{\beta\mu} \mathcal{P}_{\mu\alpha}^T \\ &\quad + M\tilde{d}_d [((x-1/2)P + p) \cdot \gamma] P_\beta \sigma_{\beta\mu} \gamma_5 \mathcal{P}_{\mu\alpha}^T \\ &\quad \left. + M\tilde{d}_u P_\beta \sigma_{\beta\mu} \gamma_5 \mathcal{P}_{\mu\alpha}^T [((x-1/2)P + p) \cdot \gamma] \right\}. \end{aligned} \quad (46)$$

In computing the vertex in Eq. (19) one must employ Fig. 5 and also its charge conjugate, the form of which is

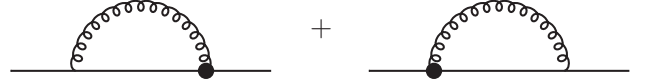


FIG. 6. Correction to the dressed-quark propagator generated by the quark chromo-EDM operator in Eq. (2). In each image the dot locates insertion of  $\mathcal{L}_{CEDM}$ .

obtained from Eq. (46) via the interchange  $\tilde{d}_u \leftrightarrow \tilde{d}_d$ , and  $p \rightarrow -p$ ,  $P \rightarrow -P$ .

## 3. $\mathcal{L}_{CEDM}$ - quark propagator

The last modification generated by the chromo-EDM term in Eq. (2) is that to the quark propagator, Fig. 6. The self-energy insertion is readily evaluated:

$$\Gamma^{S(g)} = \tilde{d}_f \frac{8}{\pi} \frac{\alpha_{\text{IR}}}{m_G^2} \mathcal{D}^{\text{iu}}(M^2) \gamma_5, \quad (47)$$

where

$$\mathcal{D}^{\text{iu}}(\omega) = \int ds \frac{s^2}{s + \omega} \rightarrow \int_{\tau_{\text{uv}}^2}^{\tau_{\text{ir}}^2} d\tau \frac{2}{\tau^3} \exp(-\tau\omega), \quad (48)$$

so that, with  $f = u, d$ ,

$$\delta_{(g)} S_f(k) = \frac{i}{k^2 + M^2} \tilde{d}_f \frac{8}{\pi} \frac{\alpha_{\text{IR}}}{m_G^2} \mathcal{D}^{\text{iu}}(M^2) \gamma_5. \quad (49)$$

## C. $\theta$ -term

Owing to a connection between the Higgs mechanism for generating current-quark masses in the SM and  $CP$  violation in the weak interaction, the effect of the  $\theta$ -term can completely be expressed through a  $U_A(1)$  rotation of the current-quark mass-matrix. We consider the  $s$ -quark to be massive and  $m_u = m_d$ , in which case the effect of the first term in Eq. (2) is expressed simply in a modification of the dressed-quark propagator:

$$S(k) \rightarrow \frac{1}{i\gamma \cdot k + M + \frac{i}{2} m \bar{\theta} \gamma_5} \quad (50)$$

$$\stackrel{m\bar{\theta} \text{ small}}{\approx} S(k) - \frac{1}{k^2 + M^2} \frac{i}{2} m \bar{\theta} \gamma_5. \quad (51)$$

### 1. Dressed-quark anomalous chromomagnetic moment

In our global-symmetry-preserving rainbow-ladder treatment of the contact interaction, the general form of the  $\rho$ -meson's Bethe-Salpeter amplitude is given in Eq. (17). The absence of a term  $\sigma_{\mu\nu} P_\nu F_\rho(P)$  is an artefact of the rainbow-ladder truncation: even using Eq. (6), a Bethe-Salpeter amplitude with  $F_\rho(P) \neq 0$  is obtained in any symmetry-preserving truncation that goes beyond



this leading order [30]. One material consequence of this omission is complete cancellation of all terms at leading-order in  $\bar{\theta}$ , so that the  $\theta$ -term's contribution to the  $\rho$ -meson's EDM is anomalously suppressed in rainbow-ladder truncation. This defect may be ameliorated by acknowledging that the dressed-quark-gluon vertex possesses an anomalous chromomagnetic moment coupling which is enhanced by dynamical chiral symmetry breaking [55]. We therefore include an effect generated by

$$\Gamma_{\mu}^{\text{acm}}(p_i, p_f) = \frac{\mu^{\text{acm}}}{2M} \sigma_{\mu\nu} (p_f - p_i)_{\nu}, \quad (52)$$

where [64]  $\mu^{\text{acm}} \sim (-1/4)$ .

In order to explicate the effect we find it convenient to first express collectively the corrections to the dressed-quark propagator computed above; viz., from Eqs. (43), (49), (51),

$$S(k) \rightarrow S(k) - i\gamma_5 \frac{\lambda}{k^2 + M^2}, \quad (53)$$

$$\lambda_{L_6} = -(1 + 2N_c) \frac{\mathcal{X}}{\Lambda^2} \frac{M}{16\pi^2} C^{\text{iu}}(M^2), \quad (54)$$

$$\lambda_{(g)} = -\tilde{d}_f \frac{8}{\pi} \frac{\alpha_{\text{IR}}}{m_G^2} \mathcal{D}^{\text{iu}}(M^2), \quad (55)$$

$$\lambda_{\bar{\theta}} = \frac{1}{2} m_{\bar{\theta}}. \quad (56)$$

Our corrections are now obtained via the diagrams in Fig. 5, except that here the dots represent Eq. (52), and one simultaneously adds the correction to one and then the other propagator. In this way, careful but straightforward computation yields

$$\begin{aligned} \Gamma_{\mu}^{\lambda, \text{acm}} &= \frac{\alpha_{\text{IR}}}{2i\pi m_G^2} \frac{\lambda^1 \mu_2^{\text{acm}} - \lambda^2 \mu_1^{\text{acm}}}{2M} \\ &\times \int_0^1 dx [C^{\text{iu}}(\omega_P) - C_1^{\text{iu}}(\omega_P)] \gamma_{\mu} \gamma_5 \\ &+ \frac{\alpha_{\text{IR}}}{6i\pi m_G^2} \frac{1}{M} \int_0^1 dx \bar{C}_1^{\text{iu}}(\omega_P) \\ &\times \left\{ 3\mu_-^{\text{acm}} \gamma \cdot (p + (x-1/2)P) \right. \\ &\quad \times [(1-x)\lambda^1 - x\lambda^2] P_{\mu} \\ &\quad + i[(1-x)\lambda^1 + x\lambda^2] [\mu_1^{\text{acm}} \gamma_{\nu} P_{\alpha} \sigma_{\alpha\mu} \\ &\quad \quad - \mu_2^{\text{acm}} P_{\alpha} \sigma_{\alpha\mu} \gamma_{\nu}] (p + (x-1/2)P)_{\nu} \\ &\quad - \lambda^{-} M [\mu_+^{\text{acm}} (p + (x-1/2)P)_{\beta} \sigma_{\mu\beta} \\ &\quad \quad \left. + 3i\mu_-^{\text{acm}} (p + (x-1/2)P)_{\mu}] \right\} \gamma_5, \quad (57) \end{aligned}$$

where  $\mu_{\pm}^{\text{acm}} = \mu_1^{\text{acm}} \pm \mu_2^{\text{acm}}$ , and  $\{\lambda^i, i=1,2\}$  represents the quark propagator correction on each leg with  $\lambda^{\pm} = \lambda^1 \pm \lambda^2$ .

One can now adapt the general expression in Eq. (57) to the particular cases of relevance herein. The first is the  $\rho$ -meson Bethe-Salpeter amplitude. Capitalising on

isospin symmetry, which entails  $\mu_u^{\text{acm}} = \mu_d^{\text{acm}} =: \mu^{\text{acm}}$ , one finds

$$\begin{aligned} \Gamma_{\alpha}^{\rho, \text{acm}} &= \frac{\alpha_{\text{IR}}}{2i\pi m_G^2} \frac{\mu^{\text{acm}} \lambda^{-}}{2M} E_{\rho} \int_0^1 dx [C^{\text{iu}}(\omega_P) - C_1^{\text{iu}}(\omega_P)] \\ &\quad \times \gamma_{\mu} \mathcal{P}_{\mu\alpha} \gamma_5 \\ &+ \frac{\alpha_{\text{IR}}}{3i\pi m_G^2} \frac{\mu^{\text{acm}}}{2M} E_{\rho} \int_0^1 dx \bar{C}_1^{\text{iu}}(\omega_P) \left\{ i[(1-x)\lambda^1 \right. \\ &\quad \left. + x\lambda^2] (\gamma_{\beta} P_{\nu} \sigma_{\nu\alpha} - P_{\nu} \sigma_{\nu\alpha} \gamma_{\beta}) (p + (x-1/2)P)_{\beta} \right. \\ &\quad \left. - 2\lambda^{-} M \mathcal{P}_{\mu\alpha} (p + (x-1/2)P)_{\nu} \sigma_{\mu\nu} \right\} \gamma_5, \quad (58) \end{aligned}$$

where “ $\lambda$ ” is constructed from the correction specified in one of Eqs. (54) – (56).

The other case is the quark-photon vertex, for which the correction is found with  $\lambda^1 = \lambda^2 = \lambda$ , since the quark flavours are identical, and we need only consider  $q^2 = 0$ :

$$\Gamma_{\mu}^{\gamma, \text{acm}} = \frac{\alpha_{\text{IR}}}{3\pi m_G^2} \frac{\mu^{\text{acm}} \lambda}{2M} \bar{C}_1^{\text{iu}}(M^2) \gamma_5 [\gamma \cdot p, \sigma_{\mu\alpha} q_{\alpha}]. \quad (59)$$

## V. $\rho$ -MESON EDM: RESULTS

### A. Analysis without Peccei-Quinn symmetry

In order to obtain a result for the  $\rho$ -meson's EDM,  $d_{\rho}$ , it remains only to sum the various contributions derived in Sec. IV as they contribute to Eq. (19), evaluated with the parameter values in Table I:

$$\begin{aligned} d_{\rho} &= -2.88 \times 10^{-3} \mu^{\text{acm}} e\bar{\theta}/s \\ &\quad + 0.785 (d_u - d_d) \\ &\quad + (1.352 + 0.775 \mu^{\text{acm}}) e(\tilde{d}_u - \tilde{d}_d) \\ &\quad - (0.091 - 2.396 \mu^{\text{acm}}) e(\tilde{d}_u + \tilde{d}_d) \\ &\quad - e \frac{s\mathcal{X}}{\Lambda^2} (2.696 - 6.798 \mu^{\text{acm}}) \times 10^{-3}. \quad (60) \end{aligned}$$

In this formula,  $d_f, \tilde{d}_f$  carry a dimension of inverse-mass and  $s = 1 \text{ GeV}$ .

A nugatory transformation allows one to rewrite Eq. (60) in terms of dimensionless electric and chromo-electric quark dipole moments; viz.,

$$\begin{aligned} d_{\rho} &= -2.88 \times 10^{-3} \mu^{\text{acm}} e\bar{\theta}/s \\ &\quad + \frac{v_H}{\Lambda^2} \left[ 0.785 (D_u - D_d) \right. \\ &\quad \left. + (1.352 + 0.775 \mu^{\text{acm}}) e(\tilde{D}_u - \tilde{D}_d) \right. \\ &\quad \left. - (0.091 - 2.396 \mu^{\text{acm}}) e(\tilde{D}_u + \tilde{D}_d) \right. \\ &\quad \left. - (1.096 - 2.763 \mu^{\text{acm}}) \times 10^{-5} e\mathcal{X} \right], \quad (61) \end{aligned}$$

where  $v_H = 246 \text{ GeV}$  is the cube-root of the phenomenological Higgs vacuum expectation value. In a class of models that includes, e.g., Ref. [65], one finds

$$D_f \sim \frac{m_f}{v_H} \sim 2 \times 10^{-5}, \quad (62)$$

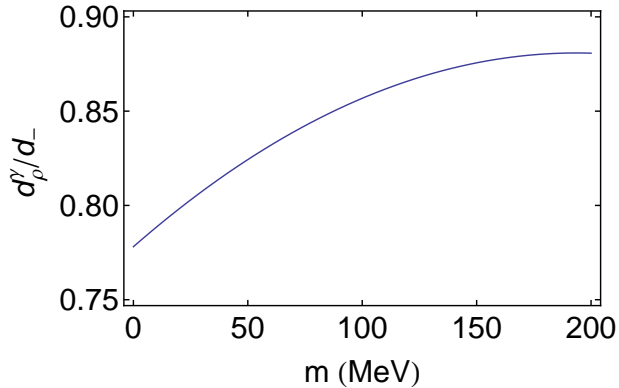


FIG. 7. Evolution of the quark-EDM component of the  $\rho$ -meson's EDM with current-quark mass, assuming  $d_-$  is independent of  $m$ .  $m = 170$  MeV corresponds to the mass of the  $s$ -quark in our treatment of the contact interaction [22], so the difference between  $d_\rho^e$  and  $d_\rho^q$  is 10%.

a result which may be used to inform expectations about the “natural” magnitude of the terms in Eqs. (60), (61).

There are four distinct types of contribution to  $d_\rho$  in Eq. (60). The first is associated with the  $\theta$ -term; and it is notable that this contribution vanishes in the absence of a dressed-quark anomalous magnetic moment, a feature which emphasises the connection between topology and dynamical chiral symmetry breaking that is highlighted, e.g., in Eq. (21) of Ref. [40]. Our result may directly be compared with that obtained in a sum rules analysis; viz.,

$$\begin{aligned} \text{herein} : & -2.9 \times 10^{-3} \mu^{\text{acm}} e\bar{\theta} \sim 0.7 \times 10^{-3} e\bar{\theta} \\ \text{Ref. [15]} : & 4.4 \times 10^{-3} e\bar{\theta}. \end{aligned} \quad (63)$$

The second contribution owes to an explicit dressed-quark EDM. It has been computed via a number of methods, so that a comparison with our results is readily compiled:

$$\begin{array}{ccccc} \text{herein} & \text{DSE [13]} & \text{BM [13]} & \text{nrQM [13]} & \text{sum rules [15]} \\ 0.79 & 0.72 & 0.83 & 1.00 & 0.51, \end{array} \quad (64)$$

where each entry is multiplied by  $d_- = (d_u - d_d)$ ; and DSE [13] summarises results obtained from momentum-dependent DSE input, BM [13] reports a bag-model result, and nrQM [13] is the non-relativistic constituent-quark value. We depict the current-quark mass dependence of this contribution in Fig. 7. It is notable that the magnitude of these results matches an existing DSE estimate of the analogous contribution to the neutron's EDM [66]. Moreover, based on Ref. [67], a perturbative analysis would yield  $2m_\rho d_\rho^{\text{pert}} = 2m d_-$ , where  $m$  is the current-quark mass. With the parameter values employed herein, this is  $d_\rho^{\text{pert}} = 0.014 d_-$ , which is just  $\sim 2\%$  of the order-of-magnitude specified by the values in Eq. (64).

The third contribution to  $d_\rho$  is generated by the quark's chromoelectric dipole moment. Its subcompo-

TABLE III. Contributions to the  $\rho$ -meson EDM associated with a quark chromoelectric dipole moment, with  $\tilde{d}_\mp^e = e(\tilde{d}_u \mp \tilde{d}_d)$ . Row 1: quark-photon vertex correction, Sec. IV B 1; Row 2:  $\rho$ -meson Bethe-Salpeter amplitude correction, Sec. IV B 2; Row 3: dressed-quark propagator correction, Sec. IV B 3; Row 4: anomalous chromomagnetic moment contributions, Sec. IV C 1; Row 5: sum of preceding four rows; Row 6: Row 5 evaluated with  $\mu^{\text{acm}} = -1/4$ ; and Row 7: sum rules result from Ref. [15], evaluated here with a heavy  $s$ -quark.

$q\gamma q$	$-0.066 \tilde{d}_-^e - 0.199 \tilde{d}_+^e$
BSA	$-0.120 \tilde{d}_-^e + 0.108 \tilde{d}_+^e$
$S(k)$	$1.538 \tilde{d}_-^e$
acm ( $\times \mu^{\text{acm}}$ )	$0.775 \tilde{d}_-^e + 2.396 \tilde{d}_+^e$
<i>our CEDM</i>	$(1.35 + 0.78 \mu^{\text{acm}}) \tilde{d}_-^e - (0.09 - 2.40 \mu^{\text{acm}}) \tilde{d}_+^e$
<i>total</i>	$1.16 \tilde{d}_-^e - 0.69 \tilde{d}_+^e$
sum rules [15]	$-0.13 \tilde{d}_-^e$

nents are detailed in Table III. The net result is comparable in magnitude and sign with that produced by the quark EDM, Eq. (64). In comparison with a sum rules computation [15], however, our result is an order of magnitude larger, has the opposite sign and contains a sizeable  $\tilde{d}_+$ -term. At least the first two of these marked discrepancies are insensitive to reasonable variations in  $\mu^{\text{acm}}$ . It is worth emphasising here that our calculation has no other variable parameters: the two specifying our model, listed in Table I, were fixed in prior studies of an array of meson and baryon observables [17–22]. This mismatch will receive further attention in future work.

The four-fermion interaction is responsible for the final contribution in Eq. (60). Its subcomponents are detailed in Table IV. As ours is the first estimate of the contribution from a dimension-six operator to the  $\rho$ -meson's EDM, there is no ready substantial comparison. On the other hand, the result in Table IV is quickly seen to be “natural” in size. The dimension-six operator is associated with a coupling  $\mathcal{K}/\Lambda^2$ , which has mass-dimension “ $-2$ ”. In order to obtain a quantity with mass-dimension “ $-1$ ”, this coupling must be multiplied by another energy scale. We are interested in an hadronic EDM, so that scale should be typical of hadron physics; e.g., the dressed-quark mass “ $M$ ”. Finally, a loop correction is required for the generation of an EDM, and loops are characterised by a factor  $1/(16\pi^2)$ . Putting these quantities together yields an expectation based on naive dimensional analysis; viz.,

$$d_\rho^{D=6} \sim e \frac{1}{16\pi^2} \frac{M}{v_H} \frac{v_H \mathcal{K}}{\Lambda^2} \sim 1 \times 10^{-5} \frac{e v_H \mathcal{K}}{\Lambda^2}, \quad (65)$$

in agreement with the magnitude of the final row in Table IV. Comparison with Eq. (62), furthermore, indicates that in our computation the quark-EDM and dimension-six contributions are naturally related via

$$d_\rho^{q\text{EDM}} \mathcal{K} \sim d_\rho^{D=6}. \quad (66)$$

TABLE IV. Contributions to the  $\rho$ -meson EDM associated with the dimension-six operator in Eq. (2). Each row should be multiplied by  $e v_H \mathcal{K} / \Lambda^2$ . Row 1: quark-photon vertex correction, Sec. IV A 1; Row 2:  $\rho$ -meson Bethe-Salpeter amplitude correction, Sec. IV A 2; Row 3: dressed-quark propagator correction, Sec. IV A 3; Row 4: anomalous chromomagnetic moment contributions, Sec. IV C 1; and Row 5: sum of preceding four rows.

$q\gamma q$	$-1.005 \times 10^{-5}$
BSA	$-9.114 \times 10^{-7}$
$S(k)$	0
acm ( $\times \mu^{\text{acm}}$ )	$2.763 \times 10^{-5} \mu^{\text{acm}}$
<i>our D = 6 total</i>	$-(1.096 - 2.763 \mu^{\text{acm}}) \times 10^{-5}$

### B. Peccei Quinn Symmetry

The leading term in Eq. (61) is that associated with  $\bar{\theta}$ . Arising from a dimension-four operator, this contribution is not suppressed by a large beyond-SM mass-scale. One may furthermore expect that, absent any symmetry to prevent it, a typical non-SM for CP-violation will produce large corrections to  $\bar{\theta}$ . In order to reconcile this with the remarkably small upper-bound on  $\bar{\theta}$  placed by the neutron's EDM, one must accept that the initial value of  $\bar{\theta}$  is very finely tuned. There is nothing to prevent this from being simply an accident of Nature. However, some view that possibility as aesthetically displeasing and prefer to introduce a new dynamical degree of freedom, the axion, a pseudo-Goldstone boson, whose role is to cancel the effect of  $\bar{\theta}$  [68]. It is notable that there is currently no empirical evidence in favour of the axion's existence and the remaining domain of parameter space is small [69].

Notwithstanding this, in the context of EDM estimates it is customary to expose the possible effect of axion physics on the results in Eq. (60) or (61). Here there is a complication. If one considers an extension of the SM with a collection of CP-odd operators that may mix with the  $\bar{\theta}$ -term, then the effective potential describing axion physics at the hadronic scale can plausibly acquire terms that shift its minimum to a nonzero value of the effective  $\bar{\theta}$ -parameter,  $\bar{\theta}_{\text{induced}}$  [7]. The quark chromoelectric dipole moment interaction is one such operator. In its case, within a sum rules calculation [15], the net effect of this mixing is elimination of  $\bar{\theta}$  in favour of a modest enhancement in magnitude of the coefficients of  $\tilde{d}_{\pm}$  in Eq. (60), with no change in sign.

The implications for our study are plain. Allowing an axion-like mechanism to play a role, then  $\bar{\theta}$  disappears from Eqs. (60) and (61), and any measurement of an hadron EDM, here that of the  $\rho$ -meson, places a little more stringent constraint on  $\tilde{d}_{\pm}$  in particular but also on  $d_{\pm}$  and  $\mathcal{K}$ .

This is, perhaps, particularly relevant to  $\mathcal{K}$ , since the high-scale physics that generates this operator will typically also produce a complex phase for the quark masses.

Within the low-energy effective theory of Eq. (2), this phase will arise from one-loop contributions to the quark propagator containing one insertion of the CP-violating four-quark operator and the quark Yukawa interaction. Consequently, constraints on  $\bar{\theta}$  imply a bound on  $\mathcal{K}$ . On the other hand, with the elimination of  $\bar{\theta}$  via an axion effective potential, the term modulated by  $\mathcal{K}$  is exposed to independent constraint [8]. Computing the contribution of the four-quark CP-violating operator to the axion potential, determining the resulting dependence of  $\bar{\theta}_{\text{induced}}$  on  $\mathcal{K}$ , and deriving the expression corresponding to Eq. (61) will be the subject of future work.

## VI. EPILOGUE

Using the leading-order in a global-symmetry-preserving truncation of QCD's Dyson-Schwinger equations, we computed the electric dipole moment of the  $\rho$ -meson,  $d_{\rho}$ , that is generated by the leading dimension-four and -five CP-violating operators and an example of a dimension-six operator. We employed a momentum-independent form for the leading-order kernel in the gap- and Bethe-Salpeter equations. This is known to produce results for low-energy pseudoscalar- and vector-meson observables that are indistinguishable from those obtained with the most sophisticated interactions available when they are analysed using the same truncation. Since the dipole moment is a low-energy observable, our predictions should be similarly reliable, in which case the framework we employ and elucidate can usefully be adapted to the more challenging task of computing the neutron's EDM,  $d_n$ .

We find that the two dimension-five operators; namely, quark-EDM and -chromo-EDM, characterised by  $d_q$  and  $\tilde{d}_q$ , respectively, produce contributions to  $d_{\rho}$  whose coefficients are of the same sign and within a factor of two in magnitude. This contrasts with an extant sum rules evaluation, in which the coefficients of the contributions have the opposite sign and differ by a factor of four in magnitude. Since all studies agree within a factor of two on the quark-EDM coefficient, the discrepancy resides with the chromo-EDM contribution. These differences invite further analysis and guarantee relevance to a DSE evaluation of the impact of  $\tilde{d}_q$  on the neutron's EDM.

Absent a mechanism that suppresses a  $\theta$ -term in any beyond-Standard-Model action, the tight constraints on the magnitude of a contribution from this term to the neutron's EDM also apply to contributions from a dimension-six four-fermion operator to this or another hadron's EDM. Should such a mechanism exist, however, we find that a dimension-six operator can match the quark-EDM and chromo-EDM in importance.

Using the techniques described herein, calculation of the neutron's EDM is underway.

## ACKNOWLEDGMENTS

We thank A. Bashir, L. Chang, C. Chen and B. H. J. McKellar for helpful comments. This work

was supported in part by: U.S. Department of Energy, Office of Nuclear Physics, contract nos. DE-AC02-06CH11357 and DE-FG02-08ER41531; Forschungszentrum Jülich GmbH; and the Wisconsin Alumni Research Foundation.

- 
- [1] E. Purcell and N. Ramsey, Phys. Rev. **78**, 807 (1950).  
 [2] A. D. Sakharov, Pisma Zh. Eksp. Teor. Fiz. **5**, 32 (1967).  
 [3] A. G. Cohen, D. B. Kaplan and A. E. Nelson, Ann. Rev. Nucl. Part. Sci. **43**, 27 (1993).  
 [4] M. Trodden, Rev.Mod.Phys. **71**, 1463 (1999).  
 [5] D. E. Morrissey and M. J. Ramsey-Musolf, arXiv:1206.2942 [hep-ph], *Electroweak baryogenesis*.  
 [6] P. Harris *et al.*, Phys. Rev. Lett. **82**, 904 (1999).  
 [7] M. Pospelov and A. Ritz, Annals Phys. **318**, 119 (2005).  
 [8] M. Ramsey-Musolf and S. Su, Phys.Rept. **456**, 1 (2008).  
 [9] S. Lamoreaux and R. Golub, J. Phys. G **G36**, 104002 (2009).  
 [10] V. Cirigliano, Y. Li, S. Profumo and M. J. Ramsey-Musolf, JHEP **1001**, 002 (2010).  
 [11] Y. Li, S. Profumo and M. Ramsey-Musolf, JHEP **1008**, 062 (2010).  
 [12] J. Kozaczuk, S. Profumo, M. J. Ramsey-Musolf and C. L. Wainwright, arXiv:1206.4100 [hep-ph], *Supersymmetric Electroweak Baryogenesis Via Resonant Sfermion Sources*.  
 [13] M. B. Hecht and B. H. J. McKellar, Phys. Rev. **C57**, 2638 (1998).  
 [14] M. B. Hecht and B. H. J. McKellar, Phys. Rev. **C60**, 065202 (1999).  
 [15] M. Pospelov and A. Ritz, Phys. Lett. **B471**, 388 (2000).  
 [16] S. Weinberg, Phys.Rev.Lett. **63**, 2333 (1989).  
 [17] L. X. Gutiérrez-Guerrero, A. Bashir, I. C. Cloët and C. D. Roberts, Phys. Rev. **C81**, 065202 (2010).  
 [18] H. L. L. Roberts, C. D. Roberts, A. Bashir, L. X. Gutiérrez-Guerrero and P. C. Tandy, Phys. Rev. **C82**, 065202 (2010).  
 [19] H. L. L. Roberts, L. Chang, I. C. Cloët and C. D. Roberts, Few Body Syst. **51**, 1 (2011).  
 [20] H. L. L. Roberts, A. Bashir, L. X. Gutiérrez-Guerrero, C. D. Roberts and D. J. Wilson, Phys. Rev. **C83**, 065206 (2011).  
 [21] D. J. Wilson, I. C. Cloët, L. Chang and C. D. Roberts, Phys. Rev. **C85**, 025205 (2012).  
 [22] C. Chen, L. Chang, C. D. Roberts, S. Wan and D. J. Wilson, Few Body Syst. *in press* (2012), [arXiv:1204.2553 nucl-th].  
 [23] L. Chang, C. D. Roberts and P. C. Tandy, Chin. J. Phys. **49**, 955 (2011).  
 [24] A. Bashir *et al.*, Commun. Theor. Phys. **58**, 79 (2012).  
 [25] C. D. Roberts, arXiv:1203.5341 [nucl-th], *Strong QCD and Dyson-Schwinger Equations*.  
 [26] P. Jain and H. J. Munczek, Phys. Rev. **D48**, 5403 (1993).  
 [27] P. Maris and C. D. Roberts, Phys. Rev. **C56**, 3369 (1997).  
 [28] P. Maris and C. D. Roberts, Int. J. Mod. Phys. **E12**, 297 (2003).  
 [29] H. J. Munczek, Phys. Rev. **D52**, 4736 (1995).  
 [30] A. Bender, C. D. Roberts and L. von Smekal, Phys. Lett. **B380**, 7 (1996).  
 [31] P. Maris, A. Raya, C. D. Roberts and S. M. Schmidt, Eur. Phys. J. **A18**, 231 (2003).  
 [32] G. Eichmann, R. Alkofer, I. C. Cloët, A. Krassnigg and C. D. Roberts, Phys. Rev. **C77**, 042202(R) (2008).  
 [33] P. Maris and P. C. Tandy, Phys. Rev. **C60**, 055214 (1999).  
 [34] M. S. Bhagwat and P. Maris, Phys. Rev. **C77**, 025203 (2008).  
 [35] S.-x. Qin, L. Chang, Y.-x. Liu, C. D. Roberts and D. J. Wilson, Phys. Rev. **C84**, 042202(R) (2011).  
 [36] S.-x. Qin, L. Chang, Y.-x. Liu, C. D. Roberts and D. J. Wilson, Phys. Rev. **C85**, 035202 (2012).  
 [37] P. Maris and C. D. Roberts, Phys. Rev. **C58**, 3659 (1998).  
 [38] P. Maris and P. C. Tandy, Phys. Rev. **C62**, 055204 (2000).  
 [39] P. Maris and P. C. Tandy, Phys. Rev. **C65**, 045211 (2002).  
 [40] M. S. Bhagwat, L. Chang, Y.-X. Liu, C. D. Roberts and P. C. Tandy, Phys. Rev. **C76**, 045203 (2007).  
 [41] G. Eichmann, I. C. Cloët, R. Alkofer, A. Krassnigg and C. D. Roberts, Phys. Rev. **C79**, 012202 (2009).  
 [42] G. Eichmann, Phys. Rev. **D84**, 014014 (2011).  
 [43] G. Eichmann, PoS **QCD-TNT-II**, 017 (2011).  
 [44] G. Eichmann and C. Fischer, Eur. Phys. J. **A48**, 9 (2012).  
 [45] M. S. Bhagwat, A. Krassnigg, P. Maris and C. D. Roberts, Eur. Phys. J. **A31**, 630 (2007).  
 [46] A. C. Aguilar, D. Binosi and J. Papavassiliou, JHEP **07**, 002 (2010).  
 [47] P. Boucaud *et al.*, Phys. Rev. **D82**, 054007 (2010).  
 [48] Y. Nambu and G. Jona-Lasinio, Phys. Rev. **122**, 345 (1961).  
 [49] D. Ebert, T. Feldmann and H. Reinhardt, Phys. Lett. **B388**, 154 (1996).  
 [50] C. D. Roberts, A. G. Williams and G. Krein, Int. J. Mod. Phys. **A7**, 5607 (1992).  
 [51] S. J. Brodsky, C. D. Roberts, R. Shrock and P. C. Tandy, Phys. Rev. **C82**, 022201(R) (2010).  
 [52] L. Chang, C. D. Roberts and P. C. Tandy, Phys. Rev. **C85**, 012201(R) (2012).  
 [53] S. J. Brodsky, C. D. Roberts, R. Shrock and P. C. Tandy, Phys. Rev. **C 85**, 065202 (2012).  
 [54] K. Nakamura *et al.*, J. Phys. **G37**, 075021 (2010).  
 [55] L. Chang, Y.-X. Liu and C. D. Roberts, Phys. Rev. Lett. **106**, 072001 (2011).  
 [56] F. T. Hawes and M. A. Pichowsky, Phys. Rev. **C59**, 1743 (1999).  
 [57] J. de Melo and T. Frederico, Phys. Rev. **C55**, 2043 (1997).  
 [58] H.-M. Choi and C.-R. Ji, Phys. Rev. **D70**, 053015 (2004).  
 [59] A. Samsonov, JHEP **0312**, 061 (2003).  
 [60] M. Bhagwat, M. Pichowsky, C. Roberts and P. Tandy, Phys. Rev. **C68**, 015203 (2003).

- [61] P. O. Bowman *et al.*, Phys. Rev. **D71**, 054507 (2005).
- [62] M. S. Bhagwat and P. C. Tandy, AIP Conf. Proc. **842**, 225 (2006).
- [63] M. S. Bhagwat, I. C. Cloët and C. D. Roberts, (arXiv:0710.2059 [nucl-th]), in *Proceedings of the Workshop on Exclusive Reactions at High Momentum Transfer*, Newport News, Virginia, 21-24 May 2007, Eds. A. Radyushkin and P. Stoler (World Scientific, Singapore, 2007).
- [64] L. Chang and C. D. Roberts, Phys. Rev. **C85**, 052201(R) (2012).
- [65] S. Weinberg, Phys. Rev. Lett. **37**, 657 (1976).
- [66] M. B. Hecht, C. D. Roberts and S. M. Schmidt, Phys. Rev. **C64**, 025204 (2001).
- [67] P. K. Pallaghy, *CP violation*, PhD thesis, University of Melbourne, 1996.
- [68] R. Peccei and H. R. Quinn, Phys. Rev. Lett. **38**, 1440 (1977).
- [69] J. E. Kim, AIP Conf. Proc. **1200**, 83 (2010).